Electronic Materials Letters, Vol. 4, No. 2 (2008), pp. 63-66

Increase of Quantum Efficiency in Organic Light Emitting Diodes with Mg-Al Alloy Cathode and RhO_2-Coated ITO Anode

Soo Young Kim, Kihyon Hong, Kisoo Kim, and Jong-Lam Lee*

Department of Materials Science and Engineering,
Pohang University of Science and Technology (POSTECH) Pohang, Kyungbuk 790-784, Korea

The enhancement of quantum efficiency using a Mg-Al alloy cathode and RhO_x-coated indium tin oxide (ITO) anode in organic light emitting diodes (OLEDs) is reported. The external quantum efficiency at a current density of 128 mA/cm^2 increased from 0.04% to 0.88% resulting from the Al cathode and ITO anode changing to Mg : Al = 8 : 2 cathode and RhO_x-coated ITO anode, respectively. The synchrotron radiation photoelectron spectroscopy results show that the work function of the ITO anode increased by 0.2 eV by coating 2 nm thick RhO_x and the work function of the Al cathode decreased by 0.4 eV by alloying the Al with Mg. Thus, both the hole and electron injection energy barriers were simultaneously lowered, which reduced the turn-on voltage and increased the quantum efficiency of the OLEDs.

Keywords: organic light emitting diodes, hole injection barrier, electron injection barrier, x-ray photoemission spectroscopy, O_2 plasma treatment.

1. INTRODUCTION

Metal/organic interfaces play important roles in the electroluminescence efficiency and stability in organic light emitting diodes (OLEDs). In order to maximize the efficiency and stability, it is important to enhance the charge injection and stability at the electrode interfaces and balance the transport of the holes and electrons. In both issues, the holes and electrons injection and interface stability are crucial. Large numbers of experimental results have demonstrated that the degradation of OLEDs is directly related to the energy barrier and interface stability at the anode.[1-2] In order to increase the stability and to enhance the external quantum efficiency, a surface-treated indium-tin-oxide (ITO) and buffer layer, such as various high work function metals, insulating materials, and oxides, deposited onto the ITO are generally used in the anode region.[3-7] In the cathode region, low work function metals, such as the alkali metal fluoride and alkali metal chloride, were used to increase the electron injection.[8-10] Thus, it is believed that the best method to increase the device performance is to promote the recombination probability via yielding a high electron and hole carrier injection into the OLED active layers at a lower driving voltage.

In a previous report, the Mg-Al alloy enhanced the electron injection because the Mg-Al alloy has a lower work function than Al.[11] The rhodium oxide (RhO_x) interfacial layer lowered the hole injection barrier without requiring a complicated process because the work function of RhO_x is higher than that of ITO.[12] Therefore, it is expected that using the Mg-Al alloy cathode with a RhO_x-coated ITO anode can simultaneously improve the electron and hole injection, which increases the external quantum efficiency.

In this letter, we report the enhancement of the external quantum efficiency in OLEDs using a Mg-Al alloy cathode and RhO_x-coated ITO anode. The RhO_x layer was prepared by exposing a thin Rh layer to O_2 plasma. The Mg-Al alloy was fabricated using a mold casting method. The change of work function was examined using a synchrotron radiation photoelectron spectroscopy (SRPES). From this, the effects of the Mg-Al alloy and RhO_x-coated ITO on the enhancement of the external quantum efficiency in OLEDs are discussed.

2. EXPERIMENTAL PROCEDURE

We prepared four samples in order to assess the hole injection properties of the RhO_x-coated ITO anode and the electron injection properties of the Mg-Al alloy cathode. A glass coating with ITO (150 nm thick, ~ 20 Ω/square) was used as the starting substrate. The ITO surface was cleaned sequentially with acetone, iso-propyl alcohol, and deionized water, and then dried with a high purity nitrogen gas. One sample used an ITO anode treated with O_2 plasma for 1 min under 100 mTorr with a power of 150 W. The other sample used a

*Corresponding author: jllee@postech.ac.kr

Table 1. Sample preparation methods for OLEDs

	OLED anodes	OLED cathodes
no-Al	ITO + O_2 plasma treatment	Mg:Al = 0:10
no-MgAl	ITO + O_2 plasma treatment	Mg:Al = 5:5
Rh-Al	ITO + O_2 plasma treatment + Rh deposition + O_2 plasma treatment	Mg:Al = 0:10
Rh-MgAl	ITO + O_2 plasma treatment + Rh deposition + O_2 plasma treatment	Mg:Al = 5:5

RhO_x-coated ITO anode. An Rh layer with a thickness of 2 nm was deposited on the plasma-treated ITO using an e-beam evaporator. The Rh film was also exposed to the O_2 plasma for 1 min to produce the RhO_x layer. These two samples were loaded into a thermal evaporator. Then, 4'-bis[N-(1-naphtyl)-N-phenyl-amino]biphenyl (α-NPD, 70 nm) and tris(8-hydroxyquinoline) aluminum (Alq_3, 60 nm) layers were deposited sequentially. Two types of cathode (100 nm) were also prepared as a function of the Mg content. The ratios of Mg to Al were 0:10 and 5:5 in weight percent, and the active area of the device was 3×3 mm^2. A summary of the sample preparation is given in Table 1. The acronyms used in Table 1 describe the OLED anodes in conjunction with the OLED cathodes. The effect of the Mg to Al ratio in the cathode on the performance of the OLED was also investigated. The current density-voltage and luminance-current density characteristics of the devices were measured.

In order to investigate the band alignment between the cathode and organic layer, Mg-Al alloys with various Mg contents were loaded into a vacuum chamber equipped with an electron analyzer in a 4B1 beam line in Pohang Acceleration Laboratory (Korea). Then, the secondary electron emission spectra were obtained using an incident photon energy of 600 eV. The photoemission onset was measured with a negative bias (-20 V) on the sample to avoid the work function of the detector.

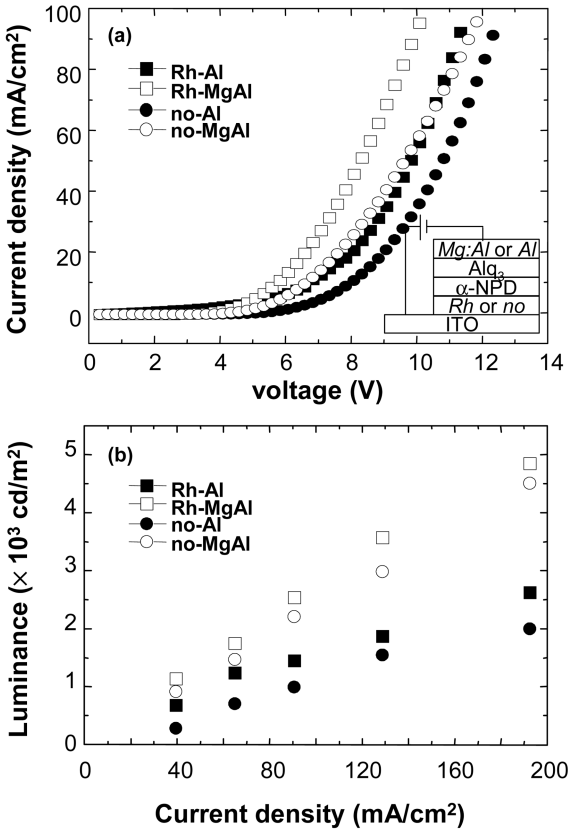

Fig. 1. (a) Current density-voltage characteristics and (b) luminance-current density characteristics of the *Rh-MgAl*, *Rh-Al*, *no-MgAl*, and *no-Al* samples. ■ : *Rh-Al*, □ : *Rh-MgAl*, ● : *no-Al*, ○ : *no-MgAl*.

3. RESULTS AND DISCUSSION

Figure 1(a) shows the current density-voltage characteristics of the four devices. The OLED structure is shown in the inset of Fig. 1(a). The operation voltages at the current density of 100 mA/cm^2 were 13 V, 12 V, 12 V, and 10 V for *no-Al*, *no-MgAl*, *Rh-Al*, and *Rh-MgAl*, respectively. The diode operation voltage significantly decreased when both the RhO_x layer and the Mg-Al alloy were used as the anode and cathodes of the OLED. The decrease in the operation voltage in the *Rh-MgAl* sample is a reflection of the simultaneous improvement in the injection of holes and electrons, resulting in the increase of the injection efficiency. The luminance-current density curves are shown in Fig. 1(b). The luminance values at the current density of 128 mA/cm^2 are 1600 cd/m^2, 3030 cd/m^2, 1920 cd/m^2, and 3620 cd/m^2 for the *no-Al*, *no-MgAl*, *Rh-Al*, and *Rh-MgAl* samples, respectively. The luminous efficiencies and external quantum efficiencies at 128 mA/cm^2 were calculated to be 0.2 cd/A and 0.04% for *no-Al*, 1.5 cd/A and 0.39% for *no-MgAl*, 1.72 cd/A and 0.42% for *Rh-Al*, and 2.85 cd/A and 0.81% for *Rh-MgAl*, respectively. In the case of *Rh-MgAl*, it is thought that the holes (electrons) were effectively injected from the anode (cathode) to the organic layer, promoting internal quantum efficiency.

Figure 2(a) displays the current density-voltage characteristics of the OLEDs as a function of the Mg content in the cathode. All devices used a RhO_x-coated-ITO anode. Also, the device structure is shown in the inset of Fig. 2(a). The operation voltages at the current density of 100 mA/cm^2 decreased from 12 V to 9.5 V as the Mg content increased from 0% to 80%. Figure 2(b) shows the luminance-current density curves. The luminance values at the current density

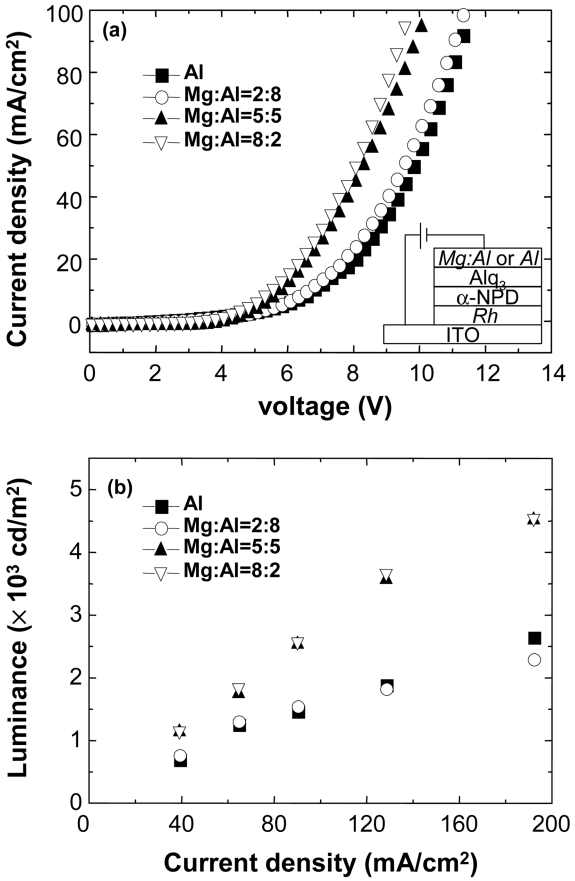

Fig. 2. (a) Current density-voltage characteristics and (b) luminance-current density characteristics of the OLEDs as a function of the Mg content in the cathode. ■ – Al, ○ – Al:Mg = 8:2, ▲ – Al:Mg = 5:5, ▽ – Al:Mg = 2:8.

of 128 mA/cm^2 are 1920 cd/m^2, 1860 cd/m^2, 3620 cd/m^2, and 3690 cd/m^2 for the OLEDs using Al, Mg:Al = 2:8, Mg:Al = 5:5, and Mg:Al = 8:2 cathodes, respectively. The luminous efficiencies and external quantum efficiencies at 128 mA/cm^2 were calculated to be 1.72 cd/A and 0.42% for Al, 1.44 cd/A and 0.38% for Mg:Al = 2:8, 2.85 cd/A and 0.81% for Mg:Al = 5:5, and 2.89 cd/A and 0.88% for Mg:Al = 8:2. This result shows that the electrons were effectively injected from the cathode to the organic layer as the Mg content increased in the cathode.

The secondary electron emission spectra for the Mg-Al alloys according to the Mg content are shown in Fig. 3. The work function was calculated considering the reported value and the change of the onset of the secondary electron spectra. The onset of the secondary electrons was determined by extrapolating two solid lines from the background and straight onset in the spectra. The work function of Al, Mg:Al = 5:5, and Mg were measured to be 4.3, 4.1, and 3.9 eV, respectively. It should be noted that the work function decreased as the ratio of Mg to Al increased.

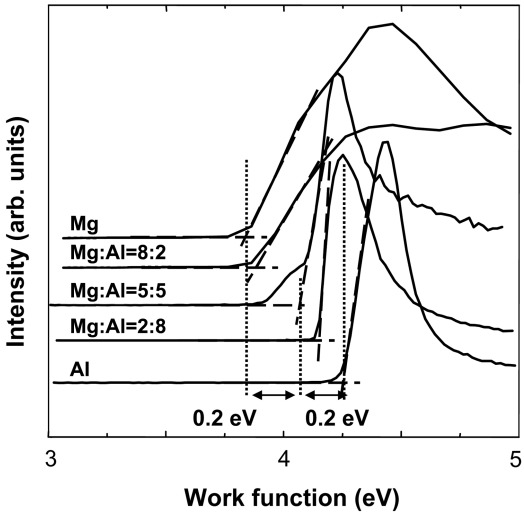

Fig. 3. Secondary electron-emission spectra for the Mg-Al alloy as a function of the Mg content. Onset of the secondary electrons was determined by extrapolating two solid lines from the background and the straight onsets in the spectra.

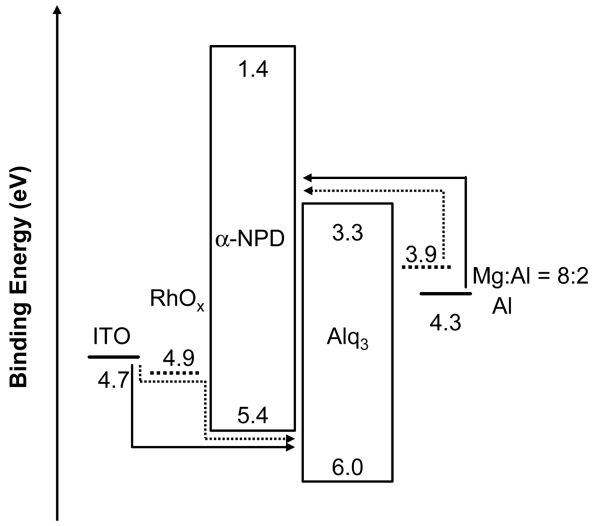

Fig. 4. Energy level diagrams of the individual device components. Work functions of the RhO_x and Mg-Al alloy were determined using a synchrotron radiation photoemission spectroscopy. The energy levels for the α-NPD and Alq_3 refer to the isolated materials and are taken from the literature.

Based on these experimental observations, the reduction in the operation voltage and the increase of quantum efficiency is explained below. When the Al cathode was replaced with the Mg-Al alloy, the current density and luminance value increased, indicating an increase of electron current density. For the Mg:Al = 8:2 cathode, the increase of quantum efficiency was maximized. This increase is explained by the energy level diagram, as shown in Fig. 4. The energy levels for ITO, α-NPD, Alq_3, and Al refer to the isolated materials and were taken from the literature.[13-16] The injection barrier

for the electrons from the cathodes to the organic materials corresponds to the energy difference between the Fermi level (E_F) of the cathodes and the lowest unoccupied molecular orbital of the organic materials. The work function of the Mg:Al = 8:2 sample was lower by 0.4 eV than that of Al, as shown in Fig. 3. Thus, the electron injection barrier between Al and Alq_3 ($\Phi_{b,e}$) decreased to $\Phi_{b,e}$ - 0.4 eV between the Mg-Al alloy and Alq_3, enhancing the recombination probability via increasing the electron injection. When the RhO_x layer was inserted between the ITO and α-NPD, the current density also increased, meaning an increase of the hole current density. The injection barrier for the holes from the anodes to the organic materials corresponds to the energy difference between the E_F of the anodes and the highest occupied molecular orbital (HOMO) of the organic materials. It has been reported that the work function of RhO_x-coated ITO is 0.2 eV higher than that of ITO.[12] Thus, it is thought that the RhO_x interlayer on the ITO moderates the discontinuity between the E_F of ITO and HOMO energy levels of the α-NPD, reducing the intrinsic hole injection barrier and increasing the hole injection. Therefore, the external quantum efficiency was maximized from 0.04% to 0.88% when both the RhO_x-coated ITO anode and Mg:Al = 8:2 cathode were used. These results show that the number of injected holes and electrons increased, showing the most improved external quantum efficiency.

4. CONCLUSIONS

In conclusion, we report the advantages of the Mg-Al cathode and RhO_x-coated ITO anode on the external quantum efficiency of OLEDs. The optimum ratio of Mg to Al is 8:2. The operation voltage of the OLEDs at a current density of 100 mA/cm^2 decreased from 13 V to 9.5 V. Furthermore, the external quantum efficiencies at 128 mA/cm^2 increased from 0.04% to 0.88%. The RhO_x-coated ITO had a 0.2 eV higher work function than the ITO and the Mg-Al sample had a 0.4 eV lower work function than Al. Thus, the RhO_x layer lowered the potential barrier for hole injection from the ITO to α-NPD and the Mg-Al cathode lowered the electron injection barrier, reducing the turn-on voltage of the OLEDs and increasing the probability of recombination.

ACKNOWLEDGEMENTS

This work was supported in part by a grant (F0004180) from the Information Display R&D Center, one of the 21st Century Frontier R&D Program funded by the Ministry of Commerce, Industry and Energy of Korean Government) and in part by the Korean Research Foundation Grant funded by the Korean Government (MOEHRD) (KRF-2005-005-J13102).

REFERENCES

1. H. Aziz and Z. D. Popovic, *Chem. Mater.* **16**, 4522 (2004).
2. S. Y. Kim, K. Y. Kim, Y.-H. Tak, and J.-L. Lee, *Appl. Phys. Lett.* **89**, 132108 (2006).
3. T.-H. Chen, Y. Liou, T. J. Wu, and J. Y. Chen, *Appl. Phys. Lett.* **87**, 243510 (2005).
4. S. A. Choulis, V.-E. Choong, M. K. Mathai, and F. So, *Appl. Phys. Lett.* **87**, 113503 (2005).
5. J. Y. Lee, *Appl. Phys. Lett.* **88**, 073512 (2006).
6. C.-C. Hsiao, C.-H. Chang, T.-H. Jen, M.-C. Hung, and S. -A. Chen, *Appl. Phys. Lett.* **88**, 033512 (2006).
7. S. Y. Kim, K.-B. Kim, Y.-H. Tak, and J.-L. Lee, *J. Appl. Phys.* **95**, 2560 (2004).
8. Y. Yi, S. J. Kang, K. Cho, J. M. Koo, K. Han, K. Park, M. Noh, C.-N. Whang, K. Jeong, and E. J. Hahn, *Appl. Phys. Lett.* **86**, 113503 (2005).
9. X. D. Feng, C. J. Huang, V. Lui, R. S. Khangura, and Z. H. Lu, *Appl. Phys. Lett.* **86**, 143511 (2005).
10. Y. Yi, S. J. Kang, K. Cho, J. M. Koo, K. Han, K. Park, M. Noh, C. N. Whang, and K. Jeong, *Appl. Phys. Lett.* **86**, 213502 (2005).
11. S. Y. Kim, W.-K. Kim, K. Y. Kim, Y.-H. Tak, and J.-L. Lee, *Electrochem. Solid St.* **9**, H1 (2006).
12. S. Y. Kim, J. M. Baik, H. K. Yu, K. Y. Kim, Y.-H. Tak, and J.-L. Lee, *Appl. Phys. Lett.* **87**, 072105 (2005).
13. D. R. Lide, *CRC Handbook of Chemistry and Physics, 83rd ed.*, p. 12-124, CRC Press, Florida (2002).
14. S. H. Chen, *J. Appl. Phys.* **97**, 073713 (2005).
15. I. G. Hill, A. Kahn, Z. G. Soos, and R. A. Pascal, Jr., *Chem. Phys. Lett.* **327**, 181 (2000).
16. Z. Y. Xie, L. S. Hung, and S. T. Lee, *Appl. Phys. Lett.* **79**, 1048 (2001).